ENERGY SPECTRA AND NUCLEAR INTERACTIONS OF COSMIC-RAY PARTICLES

N. M. KOCHARIAN, G. S. SAAKIAN, and Z. A. KIRAKOSIAN

Physics Institute, Academy of Sciences, Armenian S.S.R.

Submitted to JETP editor June 7, 1958

J. Exptl. Theoret. Phys. (U.S.S.R.) **35**, 1335-1349 (December, 1958)

Results are presented of an investigation carried out at 3200 m above sea level at the Aragats high-altitude laboratory during 1953 to 1956. The energy distributions of protons and μ mesons were measured in the range up to 100 Bev. The proton and μ-meson spectra can be approximated by the expressions $3.2 \times 10^{-3}(2+E)^{-2.8}dE$ ($E > 3$ Bev) and $0.5(5+E)^{-3}dE$ ($E > 4$ Bev) respectively. Data are given on the cross sections for inelastic nuclear interactions of high-energy π mesons and protons in graphite, copper, and lead. The inelastic nuclear interaction cross sections for protons and π mesons (σ_a) were found to be equal. The following values were found for graphite, copper, and lead respectively: $\sigma_a = 0.65\,\sigma_0$, $0.75\,\sigma_0$, and $0.9\,\sigma_0$, where $\sigma_0 = \pi(1.4 \times 10^{-13} A^{1/3})^2$ is the geometrical nuclear cross-section.

1. ENERGY SPECTRUM OF μ MESONS AT 3200 m ABOVE SEA LEVEL

THE energy spectrum of the μ mesons was determined with the magnetic spectrometer shown in Fig. 1. The accuracy of momentum measurements was higher than in the previous experiments.[1,2] The standard deviation amounted to 3, 10, 22, and 66% for 1, 5, 10, and 30 Bev/c respectively.

Protons and π mesons were distinguished from μ mesons by the nuclear interactions which they underwent in graphite absorbers A_1 to A_5 placed below the gap. The energy distribution of the μ mesons was calculated subtracting the background of nuclear active particles. The results are given in Table I.

Nuclear interactions in the absorbers placed below the gap were identified by scanning the tracks of separate particles on special diagrams, which consisted of scaled vertical cross-sections of the apparatus, parallel and perpendicular to the lines of forces (cf. Fig. 1). It was not possible to determine the particle sign for particles with 33 Bev/c momentum. For the particles of this momentum range we give therefore the total number of particles of both signs. The number 7 represents the total number of nuclear interactions of protons and π mesons with momentum > 33 Bev/c in absorbers A_1 to A_5.

The total number of μ mesons (Table I, column 8) was obtained by subtracting the number of the nuclear-active particles present in the μ-meson flux from the sum of positive and negative particles; the number of nuclear active particles was obtained in turn by dividing the number of interacting particles by the interaction probability for protons and π mesons in absorbers A_1 to A_5. The latter is given by the expression $W = 1 - \exp(-x/\lambda)$ where $x = 43$ g.cm^{-2} is the total absorber thickness, and λ is the mean free path for inelastic nuclear interactions in graphite. For protons and π mesons in the energy range $E \leq 10$ Bev, $\lambda = 95$ g-cm^{-2} (cf. Sec. 4). Accordingly, it was assumed for all momentum intervals that $W = 0.365$.

The distribution of μ mesons with respect to their deviation in the magnetic field was determined and momentum distribution was then calculated. The following relation between the particle momentum p and the deviation δ was used: $p = 5.09/\delta$. Absolute values of the differential spectrum were obtained by comparing the momentum distribution with the differential spectrum of μ mesons with $p < 14$ Bev/c found in reference 2. It was found that the ordinates of the observed momentum distribution have to be multiplied by 5.47×10^{-7} to obtain absolute values. Within the limits of the statistical errors of both experiments, the above factor is constant in the range $p < 14$ Bev/c. The ordinates of the differential energy spectrum of μ mesons are given in the last column of Table I.

The energy distribution of μ mesons was measured later again. The same array was used (cf. Fig. 1) but the graphite absorbers A_1 to A_5 were replaced by 86.2, 28.6, 47.8, 77.5 and 57 g/cm^2 of lead respectively. Accounting for the thickness of counter walls, the total amount of

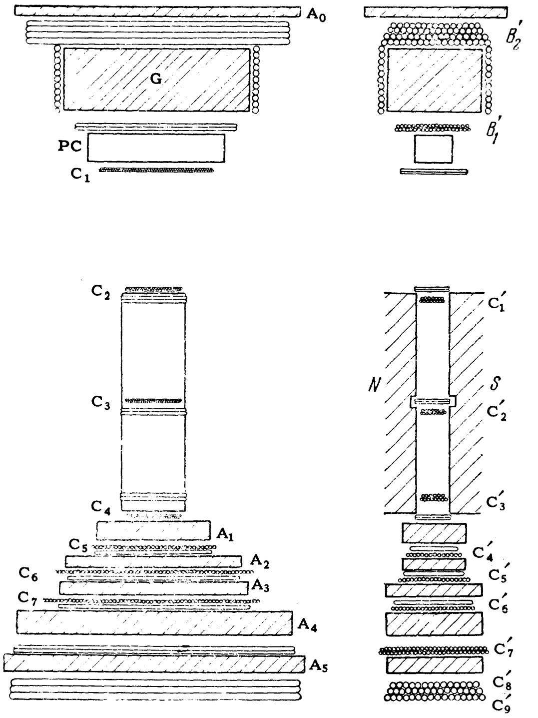

FIG. 1. Vertical cross-sections of the magnetic spectrometer, parallel and perpendicular to the magnetic lines of force. A_0) lead 32 g/cm² thick for absorption of the electron-photon component; $A_1 - A_5$ graphite, copper, or lead absorbers. $C_1 - C_4$) coordinate counter trays; G) graphite absorber; PC) proportional counter; C and B (with indices and dashes) – Geiger counter trays.

matter below the gap was equal to 300 g/cm². The results of the measurements are given in Table II. As in the first experiment, it was necessary to subtract the flux of nuclear active particles from the total flux to determine the flux of μ mesons. It was possible to find the number of nuclear interactions during the total time of observation by analyzing the particle trajectories. In this series of measurements we considered the interactions in the three first absorbers A_1 to A_5 only, the total thickness of which was 156 g/cm². In the measurements of the μ-meson spectrum, misses occurred sometimes in the last tray of counters C_9 and C_9' (counters did not fire) and we decided therefore to exclude absorbers A_4 and A_5 from consideration in order to avoid possible errors. It follows from our data (cf. Sec. 4) that, in the measured momentum range, the mean free path for inelastic nuclear interactions of protons and π mesons in lead is approximately equal to $\lambda = 195$ g/cm². The probability of an inelastic nuclear interaction in absorbers A_1 to A_3 is $W = 1 - \exp(-156/195) = 0.551$. Consequently, the actual number of protons and π mesons is equal to the ratio of the number of observed interactions to the value of the probability $W = 0.551$. The numbers of positive and negative μ mesons obtained by subtracting the background of protons and π mesons, are given in columns 8 and 9, and their total number in column 10 of Table II. The momentum distribution of the particles was calculated from the deviation distribution:

$$N(p) = N(\delta)\, d\delta / dp = \delta^2 N(\delta) / 5.09.$$

Furthermore, the ordinates of the obtained distribution were multiplied by 3.0×10^{-7} to obtain absolute values. This factor was found by comparing the measured momentum distribution with that given in reference 2. Corresponding ordinates of the differential μ mesons distribution are given in column 11 of Table II. The obtained spectrum is

TABLE I. Energy distribution of μ mesons (first experiment)

Deviation range δ, cm	Momentum range, Bev/c	Mean momentum, Bev/c	Total number of particles		Number of interacting particles		Total number of μ mesons	Ordinates of the differential μ meson spectrum cm⁻² sec⁻¹ sterad⁻¹ Bev⁻¹
			positive	negative	positive	negative		
1	2	3	4	5	6	7	8	9
2.47—2.30	2.06—2.20	2.12	416	285	21	1	641	$(2.47\pm0.09)\cdot10^{-3}$
2.30—2.14	2.20—2.38	2.30	434	325	23	0	702	$(2.30\pm0.09)\cdot10^{-3}$
2.14—1.97	2.38—2.58	2.48	456	306	18	1	710	$(1.98\pm0.07)\cdot10^{-3}$
1.97—1.81	2.58—2.82	2.70	443	322	14	2	721	$(1.70\pm0.06)\cdot10^{-3}$
1.81—1.64	2.82—3.09	2.95	476	360	12	2	798	$(1.53\pm0.05)\cdot10^{-3}$
1.64—1.48	3.09—3.45	3.27	525	366	17	2	839	$(1.35\pm0.05)\cdot10^{-3}$
1.48—1.31	3.45—3.88	3.65	527	362	20	1	832	$(1.07\pm0.03)\cdot10^{-3}$
1.31—1.14	3.88—4.44	4.10	530	375	18	2	848	$(8.42\pm0.30)\cdot10^{-4}$
1.14—0.980	4.44—5.20	4.8	574	370	15	1	900	$(6.61\pm0.20)\cdot10^{-4}$
0.980—0.815	5.20—6.25	5.7	537	367	17	1	855	$(4.50\pm0.15)\cdot10^{-4}$
0.815—0.649	6.25—7.80	7.0	528	376	12	1	869	$(2.97\pm0.09)\cdot10^{-4}$
0.649—0.484	7.8—10.4	9.0	559	327	10	2	853	$(1.76\pm0.06)\cdot10^{-4}$
0.484—0.319	10.4—16	12.7	474	293	8	2	740	$(7.60\pm0.30)\cdot10^{-5}$
0.319—0.153	16—33.2	21.5	363	203	6	2	545	$(1.94\pm0.11)\cdot10^{-5}$
0.153—0.000	33.2—∞	66.5	407		7		388	$(1.59\pm0.11)\cdot10^{-6}$

TABLE II. Energy distribution of μ mesons (second experiment)

Deviation range δ, cm	Mean momentum, Bev/c	Total number of particles		Total number of interactions		Nuclear interaction probability	Number of μ^+ mesons	Number of μ^- mesons	Total number of μ mesons	Ordinates of the differential μ meson spectrum $cm^{-2} sec^{-1} sterad^{-1} (Bev/c)^{-1}$
		positive	negative	positive $(p+\pi^+)$	negative (π^-)					
1	2	3	4	5	6	7	8	9	10	11
2.47—2.30	2.12	793	560	54	1	0.551	695	558	1253	$(2.56\pm0.07)\cdot10^{-3}$
2.30—2.14	2.39	780	539	49	2	0.551	692	536	1228	$(2.17\pm0.06)\cdot10^{-3}$
2.14—1.97	2.48	816	577	48	1	0.551	760	575	1335	$(2.03\pm0.06)\cdot10^{-3}$
1.97—1.81	2.70	837	623	49	3	0.551	747	618	1365	$(1.75\pm0.05)\cdot10^{-3}$
1.81—1.64	2.95	866	636	39	5	0.551	796	627	1423	$(1.52\pm0.04)\cdot10^{-3}$
1.64—1.48	3.27	913	668	34	3	0.551	852	663	1515	$(1.33\pm0.03)\cdot10^{-3}$
1.48—1.31	3.65	971	722	33	4	0.551	911	715	1626	$(1.13\pm0.03)\cdot10^{-3}$
1.31—1.14	4.10	983	709	30	5	0.551	931	700	1631	$(8.76\pm0.22)\cdot10^{-4}$
1.14—0.980	4.80	1017	705	29	3	0.551	965	700	1665	$(6.75\pm0.17)\cdot10^{-4}$
0.980—0.815	5.70	999	647	29	3	0.551	947	642	1589	$(4.6\pm0.12)\cdot10^{-4}$
0.815—0.649	7.0	944	642	25	5	0.551	900	633	1533	$(2.95\pm0.07)\cdot10^{-4}$
0.649—0.484	9.0	839	602	23	4	0.551	798	595	1393	$(1.65\pm0.05)\cdot10^{-4}$
0.484—0.319	12.7	707	561	20	3	0.551	670	556	1226	$(7.14\pm0.2)\cdot10^{-5}$
0.319—0.153	21.5	555	458	12	2	0.551	533	454	987	$(1.98\pm0.06)\cdot10^{-5}$
0.153 -0.0	66.5	720		7		0.551	709		709	$(1.64\mp0.06)\cdot10^{-6}$

in a good agreement with that measured in the first series of measurements. The energy distribution of the μ mesons is shown in Fig. 2. The top curve represents the integral distribution, and the lower one the differential distribution. A portion of the curve, for $E < 2$ Bev, is taken from reference 2. In the range $E > 4$ Bev the obtained energy spectrum can be accurately described by the power

$$n_{\mu}(E)\,dE = 0.5\,(E+5)^{-3}dE. \qquad (1)$$

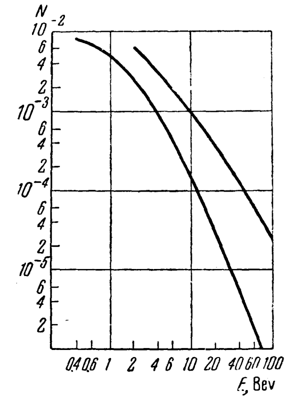

FIG. 2. Differential (lower curve) and integral (upper curve) energy spectrum of μ mesons at 3200 m above sea level. The y-axis represents the intensity N in units of $cm^{-2} sec^{-1} sterad^{-1} Bev^{-1}$ for the differential, and $cm^{-2} sec^{-1} sterad^{-1}$ for the integral spectrum.

2. ENERGY SPECTRUM OF PROTONS AT 3200 m ABOVE SEA LEVEL

The energy distribution of the protons was determined in four independent experiments.

Experiment 1. Three ordinates of the differential proton spectrum were obtained from the experimental data on the μ-meson energy distribution given in reference 2, where the experimental setup is described. In these experiments there were no absorbers above the gap, with exception of a light cover 7 g/cm^2 thick made of wood and iron. Six absorbers A_1 to A_6 were placed below the gap. The absorber A_1 was made of lead 45.2 g/cm^2 thick, the remaining ones were made of copper, 8.9, 37.4, 16, 53.4, and 17.8 g/cm^2 respectively. The relation between the particle momentum in Bev/c and their deviation in the magnetic field was $p = 7/\delta$. The projections of the trajectories of all particles were plotted on diagrams and carefully analyzed. This procedure made it possible to establish whether a particle underwent an inelastic nuclear interaction in absorbers A_1 to A_6, or traversed them without interacting. Stars, particles stopping without a visible effect, and large-angle (> 10°) scattering events were counted as interactions. Interacting particles were assumed to be protons and π^+ mesons if positive and π^- mesons if negative. The measurements were carried out during 267 hours. The number of positive particles recorded in the ranges $2.33 < p < 3.5$, $3.5 < p < 7$, and $7 < p < \infty$ Bev/c was 1650, 1715, and 1448 respectively. It was found in scanning that 160, 111, and 57 of these particles, respectively, underwent inelastic nuclear interactions. In the corresponding momentum ranges, the number of particles was 1086, 1212, and 768 respectively, of which 5, 9, and 6 underwent inelastic nuclear interactions. It is reasonable to assume that, at mountain altitudes, the number of π mesons of both signs in air is equal. The difference between the numbers of positive and negative interacting particles represents therefore the number

TABLE III. Energy distribution of protons

Deviation range δ, cm	Momentum range, Bev/c	Energy range, Bev	Mean energy, Bev	Number of particles observed	Aperture	Stopping probability	Ordinates of differential spectrum	
							Momentum cm^{-2} sec^{-1} $sterad^{-1}$ $(Bev/c)^{-1}$	Energy cm^{-2} sec^{-1} $sterad^{-1}$ Bev^{-1}
1	2	3	4	5	6	7	8	9
26—21	0.245—0.303	0.03—0.05	0.04	105	0.732	1.00	42 ± 4.1	150 ± 15
21—17	0.303—0.376	0.05—0.07	0.06	228	0.815	1.00	65.4 ± 4.3	193 ± 13
17—14	0.376—0.455	0.07—0.10	0.08	369	0.875	1.00	93.2 ± 4.9	221 ± 11
14—12	0.455—0.531	0.10—0.14	0.12	436	0.905	1.00	108 ± 5	234 ± 11
12—11	0.531—0.579	0.14—0.16	0.15	284	0.92	1.00	110 ± 6	220 ± 13
11—10	0.579—0.636	0.16—0.19	0.18	398	0.93	1.00	128 ± 6	252 ± 13
10—9	0.636—0.707	0.19—0.24	0.21	506	0.94	1.00	129 ± 6	208 ± 9
9—8	0.707—0.795	0.24—0.29	0.26	617	0.95	1.00	126 ± 5	209 ± 8
8—7	0.795—0.91	0.29—0.37	0.34	731	0.96	1.00	114 ± 6	162 ± 9
7—6	0.91—1.06	0.37—0.47	0.44	827	0.97	1.00	99.7 ± 6.3	145 ± 9
6—5	1.06—1.27	0.47—0.64	0.60	772	0.98	0.91 ± 0.04	70.2 ± 6.2	87 ± 6
5—4	1.27—1.60	0.64—0.91	0.80	562	0.99	0.66 ± 0.06	44.6 ± 3.8	54.5 ± 5.0
4—3	1.60—2.10	0.91—1.38	1.20	503	1.0	0.46 ± 0.05	37.3 ± 3.5	39.5 ± 4.4
3—2	2.10—3.20	1.38—2.38	1.9	386	1.0	0.33 ± 0.04	18.6 ± 2.9	20.5 ± 2.5
2—1	3.20—6.36	2.38—5.50	3.9	108	1.0	0.23 ± 0.04	2.53 ± 0.46	2.56 ± 0.44
1—0	6.36—∞	5.50—∞	14	13	1.0	0.14 ± 0.04	0.055 ± 0.023	0.055 ± 0.023

of protons which underwent an interaction in absorbers A_1 to A_6. According to the results of Sec. 4, the cross section for inelastic interaction of nucleons in heavy elements, in the energy range studied, amounts to $\sim 75\%$ of the geometrical cross-section. Consequently, the probability that the nucleons will interact in absorbers A_1 to A_6 is approximately equal to $1 - \exp(-x/\lambda) = 0.68$ where $x = 45.2$ g/cm^{-2} Pb + 133.5 g/cm^2 Cu = $1.52\lambda_0$ is the total absorber thickness (λ_0 is the mean free path corresponding to the geometrical cross-section of the nucleus; $\lambda = \lambda_0/0.75$ is the mean free path of inelastic interaction). The ratio of interacting protons to the interaction probability 0.68 yields the number of protons in the μ-meson flux. For the ratio of protons to μ mesons we obtained the following expressions:

$$\frac{N_p(p)}{N_\mu(p)} = \begin{cases} 0.0354 \pm 0.0041 & \text{for } \bar{p} = 14 \text{ Bev/c} \\ 0.0546 \pm 0.0045 & \text{for } \bar{p} = 4.66 \text{ Bev/c} \\ 0.0917 \pm 0.0061 & \text{for } \bar{p} = 2.8 \text{ Bev/c} \end{cases} \quad (2)$$

For particles with these momenta we find for the ordinates of the differential μ-meson spectrum $N_\mu(p)$ the values 4.7×10^{-4} and 1.74×10^{-3} respectively. Accounting for Eq. (2) we thus obtain for the ordinates of the differential energy spectrum:

$$N_p(E) = \begin{cases} (1.66 \pm 0.23)\cdot 10^{-6} & \text{for } \bar{E} = 13 \text{ Bev} \\ (3.57 \pm 0.36)\cdot 10^{-5} & \text{for } \bar{E} = 3.9 \text{ Bev} \\ (1.68 \pm 0.14)\cdot 10^{-4} & \text{for } \bar{E} = 2 \text{ Bev} \end{cases} \quad (3)$$

Experiment 2. Six copper absorbers, A_1 to A_6, with total thickness 178 g/cm^2 = $1.65\lambda_0$ were placed under the gap in this series of measurements, and 6852 protons with energy > 30 Mev stopping in the absorbers were recorded during the time of operation ($t = 1.77 \times 10^6$ sec). The energy distribution of these particles is given in Table III, column 5. Protons with $p < 1$ Bev/c stopped in the absorbers as a result of ionization losses, and those with $p > 1$ Bev/c were stopped by inelastic nuclear interactions. The last tray of counters, placed under absorber A_6, was connected in anticoincidence and only the particles which did not reach that tray, i.e., which stopped in absorbers A_1 to A_6, were recorded. Thus, from the observed number of protons with $p < 1$ Bev/c, we can construct directly the spectrum of these particles, while for the region $p > 1$ Bev/c it is necessary to know the stopping probability of the protons in absorbers A_1 to A_6 as a function of energy. This probability was found in the course of the first experiment, in which the conditions were similar with exception of an immaterial difference, namely that in the first experiment absorber P_1 was made of lead, and in the second of copper. The total thickness of absorbers A_1 to A_6, measured in units of mean free path λ_0 corresponding to the geometrical nuclear cross-section, was equal to 1.52 in the first experiment and to 1.65 in the second. As far as nuclear interactions and the stopping of particles were concerned, the physical conditions were therefore almost identical. The area of the absorbers and of the counter trays placed between them are also important, but in that respect the conditions were identical.

It was found in the first experiment that, during a total observation time, 84, 163, and 235 protons with momenta in the ranges $7 < p < \infty$, $3.5 < p < 7$, and $2.33 < p < 3.5$ Bev/c, respectively, traversed

TABLE IV. Energy distribution of protons

Momentum range, Bev/c	Mean momentum, Bev/c	Number of interactions: positive particles	Number of interactions: negative particles	Mean kinetic energy of protons	Interaction probability	Number of protons: Interacting	Number of protons: Total	Ratio of protons to μ mesons in air	Ordinates of the differential proton energy spectrum $cm^{-2}\,sec^{-1}\,sterad^{-1}\,Bev^{-1}$
1	2	3	4	5	6	7	8	9	10
2.06—2.82	2.38	76	4	1.62	0.365	72 ± 7	197 ± 19	0.071 ± 0.007	$(1.58\pm0.15)\cdot10^{-4}$
2.82—3.88	3.25	49	5	2.45	0.365	44 ± 6	121 ± 16	0.049 ± 0.006	$(6.72\pm0.82)\cdot10^{-5}$
3.88—5.20	4.45	33	3	3.6	0.365	30 ± 5	82 ± 14	0.047 ± 0.008	$(3.76\pm0.64)\cdot10^{-5}$
5.20—7.8	6.3	29	2	5.4	0.365	27 ± 4	74 ± 11	0.043 ± 0.006	$(1.68\pm0.23)\cdot10^{-5}$
7.8—16	10.5	18	4	9.6	0.365	14 ± 4	38 ± 11	0.024 ± 0.007	$(3.12\pm0.91)\cdot10^{-6}$
16—∞	32	15	(3)	31	0.48	12 ± 3	25 ± 6	0.027 ± 0.006	$(2.7\pm0.7)\cdot10^{-7}$
33.2—∞	66	7		65	0.48			0.032 ± 0.012	$(4.5\pm1.7)\cdot10^{-8}$

the array. It was found in scanning the track diagrams of interacting particles that in 12, 37, and 71 cases respectively the protons were stopped in the absorbers together with their secondary products. We find thus that the stopping probability is equal to 0.143 ± 0.044, 0.227 ± 0.041, and 0.302 ± 0.041 for $\bar{p} = 14$, 4.7, and 2.8 Bev/c respectively. The dependence of the stopping probability on momentum was plotted using these points and the point $W = 1$ for $p = 1$ Bev/c. The resulting curve was used to determine the proton stopping probability in the given experiment (cf. Table III, column 7). To calculate the ordinates of the differential energy spectrum of protons, it is necessary to divide the number of stopping protons (Table III, col. 5) by

$$S\omega t\sigma f W(E)\,\Delta E = 5.88\sigma W(E)\,\Delta E\cdot10^6, \qquad (4)$$

where ΔE is the width of the energy interval, $t = 1.77 \times 10^6$ sec is the period of observation, S is the area of the lowest counter tray, ω is the acceptance angle of the array, σ is its aperture, $f = 0.78$ is the particle detection efficiency[3] and $W(E)$ is the proton stopping probability in absorbers A_1 to A_6. In these measurements, $S\omega = 4.26$ cm^2-sterad. The ordinates of the differential momentum and energy spectra of protons are given in Table III, columns 8 and 9 respectively.

Experiment 3. The experimental data on the energy spectrum of μ mesons given in Table I contain as well all the material necessary to determine the proton energy distribution (cf. Table IV). It should be noted (cf. Fig. 1) that there is 32 g/cm^2 of lead above the array to absorb the electron-photon component. Five graphite absorbers A_1 to A_5 with total thickness equal to 43 g/cm^2 were placed under the gap. Nuclear interactions in the absorbers were identified by a careful scanning of the trajectory projections of all particles in the diagrams. The proton interaction probability in absorbers A_1 to A_5 is given in Table IV, column 6. The interaction probability is $W = 1 - \exp(-x/\lambda)$, where $x = 43$ g/cm^2 and λ is the inelastic interactive mean free path for protons. According to the data of Sec. 4, it was assumed for the first five momentum intervals that $\lambda = 95$ g/cm^2 and $W = 0.365$. For the two remaining ones ($E > 16$ Bev) it was assumed that the cross section for inelastic nuclear interactions of protons in graphite is equal to the geometrical cross section of the nucleus and, accordingly, $\lambda = 67$ g/cm^2 and $W = 0.48$. The difference between the numbers of positive (column 3) and negative (column 4) interacting particles are given in column 7 (Table IV). The total numbers of protons present in the μ-meson beam are given in column 8. These were obtained dividing the values of column 7 by the probability W. The ratio of protons to μ mesons is given in column 9. Multiplying these figures by the corresponding coordinates of the μ-meson energy spectrum,[2] we obtain the ordinates of the differential energy spectrum of the protons (column 10). For momenta ≥ 33 Bev/c it was not possible to determine the sign of the charge. A total of 388 particles, seven of which underwent an interaction, was observed in this range. We find thus, accounting for the interaction probability, that the ratio of protons and π mesons to μ mesons in the atmosphere is 0.038 ± 0.012. The relative number of π mesons at the altitude of Aragats was calculated from the production spectrum of the π mesons.[4] It was found that, at 66 Bev, the ratio of π to μ mesons at that altitude is approximately equal to 0.007. Consequently, the ratio of protons to μ mesons for $p = 66$ Bev/c is equal to 0.031 ± 0.012.

Experiment 4. Table II contains data which can be used to find the proton energy spectrum. The total number of protons and π^+ mesons $N(p + \pi^+)$ is given in column 5, and the number of π^- mesons $N(\pi^-)$ which underwent inelastic nuclear interactions in absorbers A_1 to A_3 is

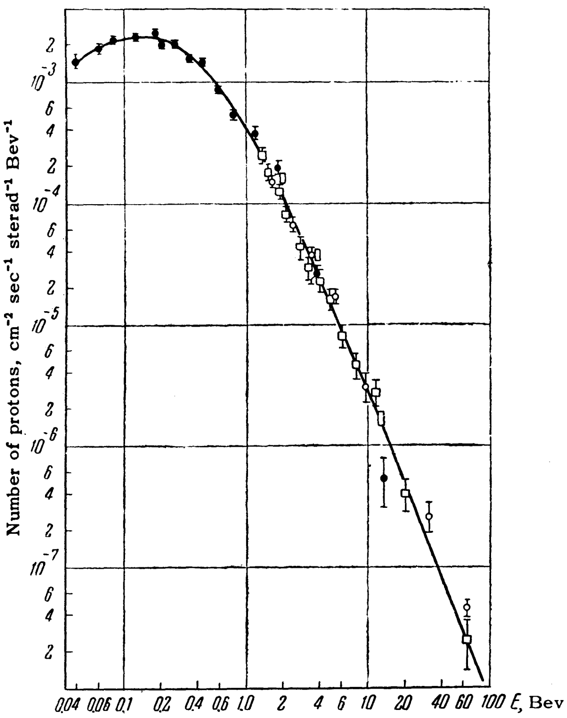

FIG. 3. Differential energy spectrum of protons at 3200 m above sea level.

listed in column 6. It was assumed, as in the previous experiment, that the number of interacting protons is equal to the difference $N(p+\pi^+) - N(\pi^-)$. To obtain the absolute number of protons which traversed the array during its operation, it was necessary to divide the number of interacting protons by the stopping probability $W = 0.551$. Further reduction of data was carried out according to the method explained in the preceding experiment. The final results are shown in Fig. 3. The ordinates of the differential proton spectrum, corresponding to experiments 1, 2, 3, and 4 are denoted by rectangles, black and white circles, and squares respectively. The energy distribution may be approximated, for $E > 3$ Bev, by the expression

$$3.2\cdot10^{-3}(2+E)^{-2.8}, \qquad (5)$$

where E is the kinetic energy of the protons in Bev.

3. ABSORPTION OF THE NUCLEONIC COMPONENT IN THE ATMOSPHERE

We shall calculate now, on the basis of the data given in the preceding section, the absorption mean free path of a vertical flux of nucleons in the atmosphere. We shall compare our data with those on the primary intensity. The geomagnetic latitude of the Aragats laboratory is 35°. The primary particle spectrum is cut off at that latitude at approximately 6.7 Bev/c. It is evident that the geomagnetic cut-off will not influence nucleon intensities for $E > 3$ Bev at mountain altitudes. One can assume that the intensities of protons and neutrons are equal in this energy range at mountain altitudes. Such an assumption is confirmed by the fact that for $E > 3$ Bev the number of proton and neutron stars in emulsions is equal within the limits of statistical error.[5-7]

The integral spectrum of primary nucleons can be approximated with a good accuracy by the formula[8]

$$N(0) = 6.1\cdot(6.34+E)^{-1.8}.$$

According to Eq. (5), the corresponding nucleon intensity at the altitude of Aragats (pressure equal to 710 g/cm^2, accounting for the small amount of matter above the array) is $N(710) = 3.56\times10^{-3}(2+E)^{-1.8}$. Consequently, the absorption mean-free-path of a vertical flux of nucleons with energy $> E$ is

$$l = 710/\ln[N(0)/N(710)] = 394/\{4.13+\ln[(E+2)/(E+6.34)]\}.$$

It follows that for nucleon energies E = 3, 5, 10, 30, 50, and 100 Bev we obtain l = 112, 108, 103, 99, 97, and 96 g/cm^2 of air, respectively. The results are in disagreement with those of references 9 to 12, where it was found that for nucleons with energy of the order of 1000 Bev, $l = 112 \pm 6$; 116 ± 9 g/cm^2 [9,12] and $l = 120$ g/cm^2.[10,11] To explain the discrepancy, one has to assume that either the nucleon intensity is too low by a factor of two or that the intensity in the primary flux is too high by the same factor, or that the errors of the spectra are such that their ratio may be wrong by a factor of two. Such an error, however, seems to us improbable. Apparently, the discrepancy is due mainly to the following reason: in the cited litera-

TABLE V. Cross sections for inelastic nuclear interactions of π^- mesons in graphite

Total energy range, Bev	Mean energy, Bev	Absorber thickness, g/cm²	Total number of π^- mesons	Number of interacting π^- mesons	Cross section σ_a, mbn
1	2	3	4	5	6
0.36–0.55	0.43	43	201	72	206^{+22}_{-25}
0.55–0.79	0.65	43	107	38	202^{+32}_{-33}
0.79–1.15	0.94	43	53	22	248^{+54}_{-57}
1.15–2.00	1.5	43	39	14	206^{+52}_{-60}
2.00–4.00	2.8	43	33	12	210^{+59}_{-68}
4.00–66.0	15	43	11	4	208^{+97}_{-120}

ture, the actual mean free path of the nuclear-active component was determined while we measured the nucleonic component. The difference may be considerable when a large amount of dense substances is present in the array.

4. CROSS-SECTIONS FOR NUCLEAR INTERACTIONS OF π MESONS AND PROTONS IN COPPER, GRAPHITE, AND LEAD

Under certain conditions, a magnetic spectrometer may be used for measurement of the total cross section for inelastic nuclear interactions of π mesons and protons with matter. For that purpose it is necessary to place an absorber over the array and, by means of Geiger-Müller counters, to detect and study the charged particles produced by neutrons in the absorber. The negative particles are π^- mesons only, and the positive ones are π^+ mesons and protons. We assume that heavy mesons do not constitute an important fraction of the number of particles. The cross section for inelastic nuclear interactions of π mesons and protons in the absorber substance can be determined by studying the nuclear interactions in the absorbers placed below the magnetic gap.

For the study of the trajectories and their interactions in the absorbers, we used scaled diagrams representing the array in two perpendicular cross sections (cf. Fig. 1). The projections of the trajectories were plotted in these planes. If a particle did not undergo a nuclear interaction, the projection of its trajectory on the plane parallel to the magnetic lines of force is a straight line passing throughout the array. The projection of the trajectory of such a particle on the plane perpendicular to the lines of force consists of a circular arc within the magnetic field, and in the absorbers outside the field — of a straight line tangential to the circle at the point where the particle left the field. When a particle undergoes a nuclear interaction in the absorbers, the following effects may be observed: (1) visible star production, (2) nuclear scattering, and (3) stopping.

Stars were defined as events in which multiple discharges were observed in counter trays placed between the absorbers. Such a criterion, however, would have been too weak, since multiple discharges could be caused by δ electrons and chance coincidences due to stray particles. Events involving δ electrons may be recognized by the fact that discharges occur always in two adjoining counters, close to the trajectory of the particle, which is then a straight line traversing all absorbers. In the majority of stars, a deviation from a straight line may be observed in at least one projection of the trajectory. In addition, for stars it is possible to construct rays intersecting in one point, and roughly the same number of rays is emitted into the upper and lower hemispheres. It is also characteristic for stars that the prongs directed backwards are generally shorter than those directed forwards, which penetrate the next absorbers, and sometimes traverse all of them. The number of chance coincidences is in general small. In addition, tracks due to these do not intersect in one point, i.e., do not form a star. In spite of the above characteristics of stars, it is sometimes difficult to decide in which absorber the interaction has occurred.

We define as nuclear scattering a deviation of one or both trajectory projections by an angle $\theta \gtrsim 10°$. At the meson energies studied, the angle of multiple Coulomb scattering is small. The above criterion is therefore sufficient for the detection of nuclear scattering events. Some of the cases assumed by us to represent nuclear scattering of mesons, could have been stars, the products of which but one were absorbed in the absorbers and did not reach the counters placed above and below the absorber in which the star was produced.

Finally, we define as particle stopping events in which the particle emerging from the magnetic field disappears in one of the absorbers. Up to that point, the particle should not undergo any interactions. A part of these events represents charge-exchange phenomena and large angle scattering events in which the particle left the apparatus. It is also possible that a star consisting of slow particles only is produced and the secondaries in the same absorber in which they were emitted. Evidently, the number of such cases tends to zero with increasing meson energy.

The cross section for nuclear interactions of π^- mesons was determined directly, since the flux of negative particles consists of π^- mesons only. The cross-section was calculated according to the formula

$$\sigma_a^{(p)} = (N_+\sigma_a^+ - N_\pi\sigma_a^{(\pi)}) / (N_+ - N_\pi), \tag{6}$$

where N_+ is the number of positive particles, N_π is the number of π^+ mesons assumed to be equal to the number of π^- mesons,[13] $\sigma_a^{(+)}$ and $\sigma_a^{(\pi)}$ are the cross sections for inelastic nuclear interactions of positive particles (π^+, p) and of π^- mesons respectively. It was assumed that $\sigma_a^{(\pi^+)} = \sigma_a^{(\pi^-)}$. This method was used for determination of the inelastic nuclear interaction cross-section of π^- mesons and protons in graphite, copper, and lead.

TABLE VI. Nuclear interactions of positive particles produced in graphite

Momentum range, Bev/c	Mean momentum, Bev/c	Absorber thickness g/cm²	Total number of particles	Number of interacting particles	Cross section σ_a, mbn
1	2	3	4	5	6
2–4	2.7	43	161	58	205 ± 27
3–4	3.3	43	59	20	191^{+41}_{-45}
4–16	6.7	43	30	11	212^{+60}_{-70}

TABLE VII. Cross sections for inelastic interactions of π^- mesons in copper

Total energy range, Bev	Mean energy, Bev	Absorber thickness, g/cm²	Total number of particles	Number of interacting particles	Cross section σ_a, mbn
0.51–0.71	0.60	29	134	33	1030^{+170}_{-157}
0.71–0.91	0.81	52	80	31	996^{+174}_{-171}
0.91–1.07	1.00	52	44	13	712^{+230}_{-269}
1.07–1.28	1.12	88.6	54	29	917^{+193}_{-163}
1.28–1.60	1.50	88.6	46	25	934^{+216}_{-176}
1.60–2.12	1.85	88.6	51	23	712^{+161}_{-139}
2.12–3.18	2.6	141.3	50	30	685^{+139}_{-121}
3.18–6.36	4.2	141.3	31	20	775^{+201}_{-165}
6.36–∞	12	141.3	35	22	742^{+183}_{-150}

(a) Cross sections for inelastic nuclear interactions of π mesons and protons in graphite. In this series of measurements five graphite absorbers A_1 to A_5, 10.1, 5.6, 7.1, 11.7, and 8.5 g/cm² respectively, were placed below the gap. The thickness given include the walls of the counters placed between the absorbers. The total thickness of walls was equal to 3 g/cm² of copper which, for nuclear interactions, is equivalent to 2 g/cm² of graphite. The π^- mesons and protons were produced by neutrons in a graphite absorber (cf. Fig. 1) 32 g/cm² thick.

Data one nuclear interactions of the negative particles (π^- mesons) are given in Table V. Standard deviations of the cross sections for inelastic nuclear interactions of π^- mesons with graphite nuclei, calculated according to the formula $\sqrt{NW(1-W)}$, where N is the number of particles and W is the interaction probability, are given in the table.

The angle of diffraction scattering in graphite is of the order of $\theta = c\hbar/Rp \sim (3.5/p)°$, where $R = 3.2 \times 10^{-13}$ cm is the radius of the graphite nucleus and p is the particle momentum in Bev/c. Large angle ($\theta \gtrsim 10°$) scattering events were also regarded as nuclear interactions. The diffraction scattering angle amounts to 8, 5, and 4° for the first three momentum ranges respectively. The measured cross-sections for these ranges, given in Table V, column 6, include therefore a certain fraction of the cross section for elastic scattering of π^- mesons. For the remaining three energy ranges the angles of diffraction scattering are sufficiently small and the given cross sections refer to inelastic interactions only. It can be seen that, for mean energies equal to 1.5, 2.8, and 15 Bev the cross section σ in graphite is constant within the limits of statistical errors, and approximately equal to $0.65\,\sigma_0$, where $\sigma_0 = 3.22 \times 10^{-25}$ cm² is the geometrical cross-section of the graphite nucleus.

Data necessary for calculating the cross-section for nuclear interactions of positive particles are given in Table VI. From a comparison of the numbers of π^- mesons and of positive particles we can conclude that protons constitute the majority of produced positive particles. The resulting cross sections given in Table VI, represent σ_a of graphite for a mixture of π^+ and p. This cross section, within experimental errors, is equal to that for π^-

TABLE VIII. Total cross sections for inelastic interactions of protons in copper

Momentum range, Bev/c	Absorber thickness g/cm²	Total number of positive particles	Number of interacting particles	Total cross section for positive particles σ_a^+, mbn	Kinetic energy range of protons, Bev	Cross section for protons σ_a, mbn
1	2	3	4	5	6	7
0.91–1.06	29	352	75	872^{+114}_{-91}	0.37–0.47	893^{+134}_{-110}
1.06–1.27	29	329	70	872^{+114}_{-108}	0.47–0.64	867^{+141}_{-133}
1.27–1.59	52	305	102	825^{+92}_{-83}	0.64–0.91	807^{+111}_{-102}
1.59–2.12	52	240	76	764^{+101}_{-84}	0.91–1.38	778^{+135}_{-113}
2.12–3.18	88.6	191	86	712^{+80}_{-73}	1.38–2.38	718^{+118}_{-107}
3.18–6.36	141.3	111	69	727 ± 90	2.38–5.5	711^{+147}_{-143}
6.36–∞	141.3	67	42	737^{+128}_{-113}	5.5–∞	738^{+334}_{-288}

TABLE IX. Cross sections for inelastic interactions of π^- mesons in lead

Total energy range, Bev	Mean energy, Bev	Absorber thickness, g/cm²	Total number of particles	Number of interacting particles	Cross section σ_a, mbn
1	2	3	4	5	6
2.65—3.98	3.18	242	37	29	1835±197
3.19—5.30	3.93	242	40	31	1960±180
3.98—7.95	5.30	242	34	26	1840±139
5.30—15.9	7.95	242	27	20	1815±197
7.95—∞	34.4	242	29	24	1810±215

mesons. One may conclude therefore that, for p = 2.7, 3.3, and 6.7 Bev/c, $\sigma_a^{(\pi)} \approx \sigma_a^{(p)} \approx 0.65\,\sigma_0$.

The graphite nucleus is therefore semi-transparent to protons and π mesons at proton energies $E \lesssim 6$ Bev.

(b) Cross sections for inelastic nuclear interactions of π mesons and protons in copper. For the determination of σ_a in copper, absorbers made of that material, 10, 18.3, 23.1, 36.4, 52.9, and 35.6 g/cm² thick, were placed below the gap. The conditions of particle selection were similar to those in the experiments with graphite. The diffraction scattering angle in copper is less than in graphite and is $\theta = (2/p)°$. The data on nuclear interactions of π^- mesons in copper are given in Table VII. It follows from these that, in the energy range above 1 Bev, the cross section for inelastic nuclear interaction is constant within the limits of experimental errors and equals $0.75\,\sigma_0$. Data necessary to determine $\sigma_a^{(p)}$ from Eq. (6) are given in Table VIII.

(c) Cross sections for inelastic nuclear interactions of π mesons and protons in lead. In these experiments interactions were studied in lead absorbers A_1 to A_5, 86.2, 28.6, 47.8, 77.5, and 57.0 g/cm² in thickness. The diffraction scattering angle for lead is $\theta = (1.4/p)°$, and the angle of multiple Coulomb scattering for the first four absorbers taken together in which the interactions were studied is approximately equal to $(5/p)°$. To exclude the contribution of Coulomb scattering we have limited our study to particles with $p \gtrsim 3$ Bev/c. All the data on nuclear interactions of π^- mesons and protons in lead are given in Tables IX and X.

Let us compare our results with the data of other workers. Lindenbaum and Yuan[14] obtained for 0.59-Bev π mesons in graphite $\sigma_a = (186 \pm 22)$ millibarns which, within the limits of experimental errors, is in a good agreement with our results. For 5-Bev π^- mesons in aluminum it was found[15] that $\sigma_a = 0.40$ barns, which amounts to ~72% of the geometrical cross section. In reference 16 it was found that $\sigma_a = 0.218$ barns in graphite at $E_\pi = 4.2$ Bev, which is close to the value obtained by us for that energy range. Our result for graphite in the high-energy range does not contradict the data of reference 16.

Data on the cross sections for inelastic interactions of protons in graphite are available in the literature for low energies only. It was found[17] that $\sigma_a = 0.25$ barns for $E = 0.87$ Bev. In references 18 and 19 it was found respectively that the cross section for 1.4-Bev neutrons in graphite is 0.200 and 0.231. Our results are in agreement with the cited works.

For copper it was found[14] that $\sigma_a = (0.73 \pm 0.11)$ barns at a total π^- meson energy of 0.59 Bev. In reference 20 it was found that $\sigma_a = 0.7$ barns at 3 Bev. For 4.2 Bev π^- mesons produced in an accelerator, it was found that $\sigma_a = 0.794$ barns.[16] The agreement is satisfactory within the limits of experimental accuracy.

Our results are not in disagreement with the

TABLE X. Cross section for inelastic interactions of protons in lead

Momentum range, Bev/c	Absorber thickness g/cm²	Total number of positive particles	Number of interacting particles	Cross section for positive particles, mbn	Kinetic energy of protons, Bev	Cross section for protons σ_a, mbn
1	2	3	4	5	6	7
3.19—5.30	242.2	157	113	1780±170	3.6	1791±220
3.98—7.95	242.2	111	84	1860±208	5.16	1850±260
5.30—15.9	242.2	64	46	1780±230	7.46	1711±300
7.95—∞	242.2	51	39	1830±280	24.6	1770±360

available data on the cross section for inelastic interactions of nucleons in copper.[17-19,21] Cross sections in lead were measured up to 970 Mev. At that energy it was found that $\sigma_a = (1828 \pm 100)$ millibarns.[22] It was found, using the Brookhaven cosmotron, that $\sigma_a = 1730$ millibarns ($\mp 5\%$) for 1.4 Bev neutrons. In another work[23] it was obtained for 860 Mev protons that $\sigma_a = (1690 \pm 900)$ millibarns. For the low-energy range we have no data to compare with the literature. It should be noted, however, that the cross sections given in Table IX and X for $E > 3$ Bev are, within the limits of statistical errors, identical with the cited values.

On the basis of the data obtained one can draw the following conclusions:

1. The cross sections for inelastic nuclear interactions of π mesons and protons in the energy range $\gtrsim 1$ Bev are, within the limits of experimental errors, equal and independent of energy.

2. If we assume that the geometrical cross section of the nucleus is $\sigma_0 = \pi(1.4 \times 10^{-13} A^{1/3})^2$, the nuclei are partially transparent for π meson and protons with $E > 1$ Bev. The transparency decreases with increasing atomic number. For graphite, copper, and lead we have $\sigma_a = 0.65\,\sigma_0$, $0.75\,\sigma_0$, and $0.9\,\sigma_0$ respectively.

[1] N. M. Kocharian, J. Exptl. Theoret. Phys. (U.S.S.R.) **28**, 160 (1955), Soviet Phys. JETP **1**, 128 (1955).

[2] Kocharian, Aivazian, Kirakosian, and Aleksanian, J. Exptl. Theoret. Phys. (U.S.S.R.) **30**, 243 (1956), Soviet Phys. JETP **3**, 350 (1956).

[3] N. M. Kocharian, Doctorate Dissertation, Phys. Inst. Acad. Sci., Moscow 1954.

[4] G. S. Saakian, Dokl. Akad. Nauk ArmSSR **24**, 3 (1957).

[5] Brown, Camerini, Fowler, Heitler, King, and Powell, Phil. Mag. **40**, 307 (1949).

[6] Camerini, Davies, Fowler, Franzinetti, Muirhead, Lock, Perkins, and Yekutieli, Phil. Mag. **42**, 1241 (1951).

[7] M. Teucher, Helv. Phys. Acta **26**, 434 (1953).

[8] P. Budini and G. Moliere, Das Zusammenspiel der Komponenten. Vortraege ueber kosmische Strahlung. Ed. by W. Heisenberg, 1953, Berlin, p. 365.

[9] K. P. Ryzhkova and L. I. Sarycheva, J. Exptl. Theoret. Phys. (U.S.S.R.) **28**, 618 (1955), Soviet Phys. JETP **1**, 572 (1955).

[10] Kaplong, Klose, Ritson, and Walker, Phys. Rev. **91**, 1573 (1953).

[11] Klose, Kaplong, Ritson, and Walker, Phys. Rev. **92**, 855 (1953).

[12] G. T. Zatsepin, Doctoral Dissertation, Phys. Inst. Acad. Sci., Moscow 1954.

[13] A. V. Khrimian, Izv. Akad. Nauk SSSR, Ser. Fiz. **19**, 700 (1955) [Columbia Tech. Transl. **19**, 638 (1955)].

[14] S. J. Lindenbaum and L. C. L. Yuan, Phys. Rev. **92**, 1578 (1953).

[15] Ilse Jr., Lagarrigue, and Pyle, Phys. Rev. **100**, 1799 (1955).

[16] Winker, Bostick, and Mayer, Bull. Am. Phys. Soc. **1**, 252 (1956).

[17] Chew, Leavitt, and Shapiro, Bull. Am. Phys. Soc. **29**, 47 (1954).

[18] Coor, Hill, Hornyak, Smith, and Snow, Phys. Rev. **98**, 1369 (1955).

[19] Snow, Coor, Hill, Hornyak, and Smith, Bull. Am. Phys. Soc. **29**, 54 (1954).

[20] Schein, Haskin, and Glasser, Nuovo cimento **1**, 131 (1956).

[21] W. O. Lock and P. V. March, Proc. Roy. Soc. **230A**, 222 (1955).

[22] Abashian, Coll, and Cronin, Bull. Am. Phys. Soc. **7**, 350 (1956).

[23] Chew, Leavitt, and Shapiro, Phys. Rev. **99**, 857 (1955).

Translated by H. Kasha
290